HHV-6A infection of endometrial epithelial cells affects immune profile and trophoblast invasion

Running title: HHV-6A infection and endometrial immune profile

Daria BORTOLOTTI[1], Valentina GENTILI[1], Antonella ROTOLA[1], Rosario CULTRERA[2], Roberto MARCI,[3,4], Dario DI LUCA[1], Roberta RIZZO[1]

[1]University of Ferrara, Department of Medical Sciences, Section of Microbiology and Medical Genetics, Ferrara, Italy; [2]University of Ferrara, Department of Medical Sciences, Section of Dermathology and Infective Medicine, Ferrara, Italy; [3]University of Ferrara, Department of Morphology, Surgery and Experimental Medicine, Section of Orthopedics, Obstetrics and Gynecology and Anesthesiology and Reanimation Ferrara, Italy; [4]University of Geneva, School of Medicine, Geneva, Switzerland.

Corresponding author:

Roberta Rizzo

Department of Medica Sciences – Section of Microbiology - University of Ferrara

Via Luigi Borsari, 46 - 44121 Ferrara (Italy)

Tel: 00390532455382; e-mail: rbr@unife.it

Acknowledgements: We thank Iva Pivanti for her excellent technical assistance, and Linda Sartor for revising the English manuscript. This work was supported by HHV-6 Foundation grant (PI: Roberta Rizzo), Ricerca Finalizzata GR-2011-02346947 (PI: Roberta Rizzo); FISM-Fondazione Italiana Sclerosi Multipla grant (PI: Roberta Rizzo, cod 2015/R/20). All the authors have no conflict of interest to declare.

Abstract

Problem: We first reported Human herpesvirus (HHV)-6A DNA presence in 43% of endometrial cells from women with idiopathic infertility, whereas no fertile control women harbored the virus. We investigated the effect of HHV-6A infection on the immunological status of the endometrium.

Method of study: Endometrial biopsies, uterine flushing, and whole blood samples were collected from 67 idiopathic infertile women (mid-secretory phase). We analyzed the endometrial immunological status evaluating: i) the effect of HHV-6A infection on endometrial immune profile analyzing the ratio of Interleukin (IL)-15/ Fibroblast growth factor-inducible 14 (Fn-14) and IL-18/ TNF-related weak inducer of apoptosis (TWEAK) mRNA as a biomarker of endometrial (e)Natural killer activation/maturation, angiogenesis, and Th1/Th2 balance; ii) endometrial receptivity to trophoblasts in endometrial 3D in vitro model; iii) Natural killer (NK) cells and T cells percentage and subpopulations by flow cytometry.

Results: We confirmed the presence of HHV-6A infection in a 40% of idiopathic infertile women, characterized by an immune profile reflecting eNK cell cytotoxic activation and a decrease in CD4+CD25+CD127dim/- regulatory T cells. The co-culture of endometrial epithelial cells with spheroids generated from the extravillous trophoblast-derived cell line JEG3 showed a 2-fold expansion of spheroids on endometrial epithelial-stromal cells (ESC) culture surface from HHV-6A negative women while no expansion was observed on the surface of ESC from HHV-6A positive women.

Conclusions: The identification of an effect of HHV-6A infection on endometrial immune status opens new perspectives in idiopathic infertile women care management. In addition, it would be possible to select antiviral therapies as novel, non-hormonal therapeutic approaches to those idiopathic infertile women characterized by the presence of endometrial HHV-6A infection, to increase their pregnancy rate.

Keywords: idiopathic female infertility; NK cells; T cells; HLA-G

Introduction

It is believed that the impairment of endometrial receptivity can be a major cause of primary idiopathic infertility, a phenomenon that occurs with the failure of implantation. We have previously associated the positivity for HHV-6A infection of endometrial epithelial cells with primary infertility [1]. Human herpesvirus 6 (HHV-6) is an ubiquitous pathogen of the Betaherpesvirinae subfamily, which primarily infects CD4+ T cells [2]. Similarly to other herpesviruses, HHV-6 remains in latency into the host, after an initial productive infection [3]. HHV-6 is a set of two related viruses known as HHV-6A and HHV-6B [4]. Even if these two viruses present a similar genetical sequence, they differ for biological and pathogenic characteristics. HHV-6B causes exanthema subitum in young children [5]. HHV-6A seems to be involved in other pathologies, such as multiple sclerosis [6] and encephalitis [7]. Moreover, we have recently shown the presence of HHV-6A, but not HHV-6B infection in endometrial epithelial cells of a subgroup of idiopathic infertile women [1]. HHV-6 infection is implicated in immune-regulation: i) direct infection and induction of apoptosis of CD4+ T lymphocytes [8 9]; ii) lysis of cytotoxic leukocytes (CD8+ T cells, NK cells) [10,11]; iii) block of dendritic cells and macrophages maturation [12 13]; iv) inability of macrophages and dendritic cells to produce IL-12p70 after interferon gamma induction [13-15]; v) dysregulation of cytokine networks, with increased secretion of IL-10, RANTES, TNF-alpha and IL-1beta [16]; vi) decreased expression of CD14, CD64 and HLA-DR on the surface of monocytes as a mechanism of immune evasion [17].

The embryo implantation is influenced by local and systemic immune responses involving immunoglobulins, cytokines, hormonal and other endometrial factors. A synergism of these factors is critical for successful implantation and subsequent conception. In particular, Natural killer (NK) cells, regulatory T cells (Treg) and cytokines have been implicated to play a role in female reproductive performance [18-20]. NK cells are a type of large granular lymphocyte that belong to the innate immune system. NK cells cause cytotoxic effects by inducing lysis or apoptosis of the target cells mediated by the release of granular components within their cytoplasm (perforin, granzymes) or secretion of cytokines, such as tumour necrosis factor-alpha, interleukin (IL)-10, interferon-gamma

and transforming growth factor-beta. Uterine NK cells are adjacent to trophoblast cells, and thereby considered as one of the important players behind maternal acceptance of the fetus. Decidual NK cells have generally reduced cytotoxicity, promote vascular formation of spiral arteries and allow trophoblast invasion through various cytokine secretion, including macrophage colony-stimulating factor (M-CSF) and granulocyte macrophage-colony stimulating factor (GM-CSF) [29]. Additionally, the secretion of growth-promoting factors from NK cells has shown to be essential for fetal growth [30]. Uterine NK cells have a unique receptor repertoire, expressing killer-cell immunoglobulin-like receptors (KIRs) and immunoglobulin-like transcript-2 (ILT2), and lack NKp30, one of the natural cytotoxicity receptors (NCRs) known to be expressed in peripheral blood NK cells [27], [42]. Some of the KIRs are receptors for HLA-G and HLA-C; both are surface antigens on trophoblast cells and are implicated inthe maintenance feto-maternal tolerance.

The T cell population in the endometrium consists of different subsets, including regulatory CD4+CD25+ T cells (Tregs) [52]. The Treg subset develops in the thymus and peripheral tissue, infiltrates the endometrium and functions by e.g. secreting immunosuppressive cytokines to prevent the immune system activation. Tregs are essential for successful pregnancy, protecting the semi-allogenic fetus from immune rejection [56]. One study reported that soluble HLA-G (HLA-G5), secreted by human mesenchymal stem cells, induced CD4+CD25+FoxP3+ regulatory T cells [60], suggesting a local induction of Treg proliferation and differentiation in relation to pregnancy. HLA-G is a nonclassical MHC class I antigen with very little sequence variability [21]. It is expressed as membrane-bound molecule (HLA-G1-3) and soluble molecule (HLA-G5-7) obtained by mRNA alternative splicing. It is not expressed in normal tissues except in trophoblasts from early gestation placentas [22]. HLA-G exerts multiple immunoregulatory functions such as inhibition of natural killer (NK) cell or T-cell-mediated cytolysis, induction of T-cell apoptosis, or inhibition of trans-endothelial NK cell migration. Since the net result of these effects is immunosuppression, HLA-G expression in fetal-maternal interface may favor implantation and pregnancy outcome [23]. The specific interaction between KIR2DL4 and HLA-G leads to the secretion of pro-angiogenic factors as VEGF from eNK

cells [24]. Similarly, NK cells are controlled by HLA-E molecules. HLA-E functions as ligand for CD94-NKG2 receptors and has a peptide-binding groove that is ideally suited for binding peptides derived from the leader sequences of other MHC-I molecules [25]. In this regard, the loss of leader-peptide loaded HLA-E expression is a marker for cells having lost expression of HLA class Ia molecules, which targets these cells for recognition and lysis by NK cells.

Another important factor implicated in the maintenance of pregnancy is the cytokine secretion and the Th1/Th2 balance. Helper T cells are classified as Th1 or Th2 according to their cytokine secretion profile. Th1 cells produce especially IL-2, INF-γ, and TNF-α. In contrast, Th2 cells produce IL-4, IL-5, and IL-10. With the onset of pregnancy, the local endometrial immune system seems to switch to an immunity dominated by a Th2 environment. This switch is believed to reduce eNK cell cytotoxicity, but also eNK cells have been reported to facilitate the Th2 immune environment [20]. Recently, the endometrial immune profile has been evaluated on the basis of the ratio of IL-15/Fn-14 mRNA as a biomarker of eNK cell activation/maturation (together with the eNK cell count) and the IL-18/TWEAK mRNA ratio as a biomarker of both angiogenesis and the Th1/Th2 balance [26]. An imbalance of this ratio might explain one of the mechanisms behind unexplained infertility.

Understanding the complex mechanisms by which extravillous trophoblast (EVT) are not able to invade the uterine lining may be considered as one of the primary aim in women with reproductive dysfunctions including infertility. One mechanism could be the presence of HHV-6A infection, that can alter the immune cell interactions at the feto-maternal interface during implantation. Therefore, to explain how HHV-6A infection can affact the maternal immune system, we have to consider a more complex interaction and cooperating immunological network. In this manuscript, we have evaluated the modification in NK and T cells immunephenotype, HLA-G and HLA-E expression in the endometrium of idiopathic infertile women.

Materials and Methods

Clinical samples

Endometrial speciments were obtained from patients admitted for tubal patency assessment by Hystero-sono contrast sonography at secretory stage of the menstrual cycle.

The endometrial sampling was performed by the Pipelle device. The Pipelle (Endocurrette, Midvale, Utah, USA) was introduced without performing cervical dilatation and withdrawn outside the uterus with a rotatory movement to get the sample that was mantained in HEPES-buffered Dulbecco modified Eagle medium/ Hams F-12 (DMEM/F-12; Invitrogen, Carlsbad, CA) with 1% antibiotic-antimycotic solution (final concentrations: 100 μg/ml penicillin G sodium, 100 μg/ml streptomycin sulfate, 0.25 μg/ml amphotericin B; Invitrogen), and 5% newborn calf serum (NCS; CSL Ltd., Parkville, VIC, Australia), stored at 4°C, and processed within 2 hrs.

We selected women with these characteristics: 21–38 years old, regular menstrual cycle (24–35 days), body mass index (BMI) ranging between 18 and 26 Kg/m2, FSH (day 2-3 of the menstrual cycle) <10 mUI/mL, 17-β-Estradiol < 50 pg/ml (day 2–3 of the menstrual cycle), normal karyotype. Women that presented endometritis, endometriosis, tubal factor, ovulatory dysfunction, anatomical uterine pathologies and recurrent miscarriage were excluded.

Ethics Statement

This study was approved by the "Ferrara Ethics Committee" and we collected written informed consent from all subjects. All subjects gave written informed consent in accordance with the Declaration of Helsinki.

Preparation of endometrial epithelial and stromal cells

The endometrium was prepared as previously described [1]. Cell dissociation was performed in Ca2+ and Mg2+ free phosphate buffered saline (PBS, pH 7.4) additionated with 300 μg/ml collagenase type III (Worthington Biochemical Corporation, Freehold, NJ) and 40 μg/ml deoxyribonuclease type I (Roche Diagnostics, Mannheim, Germany) in a shaking incubator (Bioline 4700; Edwards

Instrument Company, Narellan, NSW, Australia) rotating at 150 rpm at 37°C. Every 15 minutes, the digested tissues were homogenized vigorously and dissociation was checked microscopically. After 45 min, the digests were filtered using a 40-µm sieve (Becton Dickinson Labware, Franklin Lakes, NJ) to obstain a single cells suspension without debris. The digestion process was stoped by the addition of HEPES-buffered DMEM/F-12 containing 5%FCS. We isolated the different endometrial cellular components (mononuclear, stromal and epithelial cells) by centrifugation for 8–10 min at 390 × *g* on Ficoll-Paque (Pharmacia Biotechnology, Uppsala, Sweden). Endometrial cells were collected from the Ficoll-Paque-medium interface using BerEP4-coated magnetic Dynabeads (Dynal Biotech, Oslo, Norway) positive selection system. The sorted epithelial cells were recovered using a magnetic particle collector (Dynal Biotech) and washed in HEPES-buffered DMEM/F-12/1%FCS. The collected cells were finally seeded on culture plates coated with basement membrane extract (BME) (Matrigel®, Collaborative Biomedical Products, Bedford, MA, USA). The fraction containing mononuclear and stromal cells were collected and seeded on 100 mm plastic tissue culture dishes. After 12hrs, the supernatant cells were collected from the culture, to recover non adherent mononuclear cells. Purity of epithelial and stromal components was morphologically evaluated by light microscopy and assessed by cytokeratin-18 (CK18) and vimentin staining for epithelial and stromal cells respectively. The purity reached for each cell population was routinely over 98%.

DNA analysis

DNA extraction and analysis was performed as previously described [27]. Real time quantitative (qPCR) specific for the U94 gene were used to determine HHV-6 DNA presence and load. Samples in which 1 µg of cell DNA harbored more than 100 copies of viral DNA, were considered positive. Human RNase P or beta-actin house-keeping genes were used as a control. Real-time PCR for HHV-6 DNA was performed with the following set of primers/probe: HHV6 U94(+) (5′-GAG CGC CCG ATA TTA AAT GGA T-3′); HHV6 U94(−) (5′-GCT TGA GCG TAC CAC TTT GCA-3′); HHV6

U94 PROBE (5′-FAM-CTG GAA TAA TAA AAC TGC CGT CCC CAC C-TAMRA-3′). The standard curve was generated by amplification of a plasmid containing the targeted HHV-6 sequences. The method had a 6-log dynamic range and a sensitivity of 20 copies/mL. All clinical samples were randomly and blindly investigated. Furthermore, when enough material to repeat the analysis was present, the analysis was repeated again in a randomized and blinded fashion at a distant time from the first analyses. HHV-6A or B identification was performed as reported previously [27], by restriction enzyme digestion of the U31 nested PCR amplification product and visualition of the digestion products on ethidium bromide stained agarose gel after electrophoresis migration.

RNA analysis

RNA cell extraction was performed using the RNeasy kit (Qiagen, Hilden, Germany). Extracted RNA did not contain contaminant DNA, as assured by DNase treatment and control β-actin PCR without retrotranscription reverse transcription [28]. RNA reverse transcription was performed by the RT2 First strand kit (Qiagen, Hilden, Germany). The cDNAs were stored at –20°C until use.

Quantitative RT-PCR

Quantitative RT-PCR was performed with a Applied Biosystems™ 7500 Fast Real-Time PCR System and SYBR Green Master mix (Applied Biosystems; USA). Final concentrations for reaction setup were 0.5 µm of sense and antisense primers and 1/20 of diluted cDNA. Cycling conditions were as follows: denaturation (95°C for 5 min), amplification, and quantitation (95°C for 10 s, 60°C for 10 s, and 72°C for 15 s) repeated 40 times, a melting curve program (65–95°C with a ramp rate of 2.2°C/s), and a cooling step to 4°C. Primer sequences are detailed in Ledee et al [26]. Each quantitative RT-PCR assay included a solution without cDNA and inter-run calibrator (IRC) samples as negative and positive controls [26]. The IRC was obtained from pools of PHA (phytohaemagglutinin A)-stimulated lymphocytes for TWEAK, Fn-14, RPL13A, and beta-2-microglobulin (β2M) and from the endometrial sample for IL-18 and IL-15. The IRC cDNA, after dilution by a factor of 20, underwent the same quantitative RT-PCR protocol as the unknown samples. PCR efficiency for each quantified

target and reference was calculated with known serial dilutions of each specific cDNA. DataAssist software (Applyed Biosystems) was used to analyze data, and each specific target transcription level was normalized to the geometric mean of the transcription level of the reference gene. Gene amplification efficiency was specifically determined. For each sample, the results were expressed as the ratio of target/reference cDNA.

eNK cell purification

Endometrial NK cells were separated from endometrial leukocyte samples using the negative magnetic cell separation (MACS) system (Miltenyi Biotech, Gladbach, Germany) [1]. The analysis of purified cell fraction by flow cytometry with CD3-PerCp-Cy5.5, CD56-FITC moAbs (e-Bioscience, Frankfurt, DE), demonstrated that the NK cell content was >90% (data not shown). Freshly purified NK cells were cultured for 24 h in presence of suboptimal doses of IL-12 (1 ng/ml).

Flow cytometry

eNK cells were labeled with fluorophore-conjugated antibodies: CD3-PE-Cy7, CD16-PE, CD56-APC (BD, Italy).

PBMCs were extracted by Ficoll-Paque (Pharmacia Biotechnology, Uppsala, Sweden) and analyzed for immunephenotype: T cells: CD3-AmCyan (Clone SK7), CD4-PE (Clone S3.5), CD8-PECy7 (Clone: RPA-T8), CD25-PerCPCy5.5 (Clone PC61.5), CD127-APCCy7 (Clone A7R34) monoclonal antibodies; B cells: CD19-APC (Clone SJ25-C1), HLA-DR-FITC (Clone LN3) monoclonal antibodies; NK cells: CD3-AmCyan (Clone SK7), CD19-APC (Clone SJ25-C1), CD16-APCCy7 (Clone B73.1), CD56-PE (Clone CMSSB) monoclonal antibodies. Anti-isotype controls (Exbio, Praha, Czech Republic) were performed. Data were analyzed using FACS CantoII flow cytometer (BD, Milan, Italy) and FlowJo LLC analysis software (Ashland, Oregon, USA). Ten thousand events were acquired.

JEG3 cell spheroids

The human JEG-3 choriocarcinoma cell line (ATCC HTB-36) was used for attachment assays. Cell spheroids were generated in complete RPMI medium additioned with 1.5% agarose, obtaining 100–250 μm diameter spheroids at 2- 4 days of culture, using $3x10^4$ cells/ml medium [29].

For attachment assays, JEG-3 spheroids were transferred onto endometrial epithelial-stromal cells (ESC), prepared in a 1:1 ratio, from HHV-6A positive and negative women, one by one with a fine Pasteur pipette. After 2, 3 days of incubation, the attachment rate was calculated by the Syto59 (Thermo Fisher Scientific, USA), under fluorescence microscopy, to visualize the modification in spheroid contours in comparison with the beginning of the observation period (T0). The ratio between T3 and T0 area, calculated by Nikon Nis-Elements (Nikon Italy) was used to evaluate the modification in spheroid dimensions.

Immunofluorescence assay

HLA-G and MUC-1 expression was analized by immunofluorescence with FITC anti-human HLA-G (Clone 87G)and PE anti-human CD227 (MUC-1) Ab (Clone 16A) (Biolegend, CA, USA), as previously described [1].

Western Blot analysis

Proteins were obtained by cell lysis with ReadyPrep Protein Extraction Kit (Bio Rad, Segrate, MI, Italy) and the concentration was quantified by means of the Bradford assay (Bio Rad) using bovine albumin (Sigma-Aldrich, S.Louis, MO, USA) as standard. Twenty μg of total proteins were analyzed in denaturating conditions in 10% TGX-Pre-cast gel (Bio Rad), with subsequent electroblotting transfer onto a PVDF membrane (Millipore, MA, USA) [30]. The membranes were incubated with mouse anti-Human CD227 Moab (Biordad) for MUC1 detection, or mouse monoclonal 4H84 to

HLA-G Moab and with a horseradish peroxidase (HRP)-conjugated antimouse antibody (1:5000; Amersham Biosciences, NJ, USA) and then developed with the ECL kit (Amersham Biosciences, NJ, USA). The images were acquired by Gel Doc XR+ System (Bio Rad).

Statistical analysis

Data were analyzed by Student T test and Fisher exact test (Stat View software (SAS Institute Inc)). Statistical significance was assumed for $p<0.05$ (two tailed).

Results

HHV-6 in clinical specimens

We enrolled 67 idiopathic infertile women and 100 fertile women with at least one previous successful pregnancy. As reported in **Table 1**, the two cohorts presented no significant differences.

The endometrial biopsies were analyzed for the presence of HHV-6 infection in epithelial and stromal cells fractions. Purity of epithelial and stromal components was morphologically evaluated by light microscopy and assessed by cytokeratin-18 (CK18) and vimentin staining for epithelial and stromal cells respectively (**Supplementary Figure 1A**). As reported in **Table 2**, we found HHV-6B DNA in the peripheral blood mononuclear cells of the 25% and 24% of idiopathic infertile women and control women, respectively (p=0.856; Fisher exact test). These results confirmed the previously reported frequency of the HHV-6B virus in a 25-30% of peripheral blood samples [1]. On the contrary, HHV-6A DNA was not revealed in the peripheral blood of all the subjects. Forty percent (27/67) women with idiopathic infertility were positive for HHV-6A DNA in their endometrial epithelial cells, while fertile women did not present HHV-6A viral DNA in their endometrial epithelial cells ($p<0.0001$; Fisher exact test). HHV-6B DNA was not present in all the endometrial biopsies, as previously reported [1].

The average viral load in endometrial epithelial cells from HHV6-A positive infertile women was 520.000 copies/ug of cellular DNA (range 710.000–189.000 copies/ug DNA), corresponding to about 4 copies of viral DNA per diploid cell (**Table 2, Supplementary Figure 1B**).

Effect of HHV-6A infection on endometrial immune profile

On the basis of the results previously obtained on the ratio of IL-15/Fn-14 mRNA as a biomarker of uNK cell activation/maturation and the IL-18/TWEAK mRNA ratio as a biomarker of both angiogenesis and the Th1/Th2 balance [26], we evaluated the immune profile in our women (**Table 3**). We considered the presence of a modification in the immune-profile when a parameter is below (low immune activation) or above (high immune activation) 2SD of the values observed in fertile women group, used as control. The IL-15/Fn-14 and IL-18/TWEAK mRNA ratio were considered as previously reported [26]. In particular, an IL-18/TWEAK mRNA ratio was considered low when below

0.03 (mean −1 SD) and high when >0.12 (mean + 1 SD), while an IL-15/Fn-14 mRNA ratio was considered low when below 0.3 (mean −1 SD) and high when >3 (mean + 2 SD). We observed a low immune activation profile in HHV-6A negative infertile women, characterized by a low IL-15/Fn-14 mRNA expression, reflecting a low eNK maturation and a low local IL-18/TWEAK mRNA ratio, reflecting a low local angiogenesis. On the contrary, HHV-6A positive infertile women presented an over-activated immune-profile, with high IL-15/Fn-14 and IL-18/TWEK mRNA expression, representative of eNK cell cytotoxic activation.

As a proof of concept, we evaluated the immune phenotype of eNK cells. We observed a lower percentage of $CD56^{bright}CD16^{-}$ (e)NK cells in women positive for HHV-6A infection ($p<0.01$) (**Figure 1A, Supplementary Figure 1C** as previously observed [31] and in agreement with immune-profile results (**Table 3**), while no differences in the cytotoxic $CD56^{dim}CD16^{-}$ eNK cells (**Figure 1A**). When we looked at peripheral blood cell subsets, we observed no differences in the percentage of T, B and NK cells (**Figure 1B**). On the contrary, when we evaluated the immune-phenotypes, we observed a decrease in $CD4^{+}CD25^{+}CD127^{dim/-}$ regulatory T cells in women positive for HHV-6A infection ($p<0.01$) (**Figure 1C**).

Effect of HHV-6A infection on endometrial receptivity to trophoblast invasion.

To assess the effect of HHV-6A infection on endometrial receptivity, we set up an *in vitro* model of implantation by co-culturing endometrial epithelial cells with spheroids generated from the EVT-derived cell line JEG3.

A co-culture model was established to mimic the trophoblast– decidual interface in early pregnancy. Spheroids were formed from the trophoblast cell line JEG-3 and placed onto a monolayer of epithelial-stromal cells in a 1:1 ratio (ESC) from HHV-6A positive and negative women. For comparison, spheroids were plated in the absence of ESC. The area covered by each individual spheroid was determined at the beginning and at the end of the co-culture period. To visualize the spheroid contours, Syto 59 staining for the JEG3 spheroids was performed at the beginning of the

observation period (T0) (**Figure 2**) Within 3 days (T3), spheroids on ESC culture surface from HHV-6A negative women expanded 2-fold while spheroids on ESC culture surface from HHV-6A positive women failed to expanded. Meanwhile, we evaluated if the co-culture of ESC with trophoblast spheroid impact on trophoblast molecular expression. We analyzed the expression of HLA-G and mucin-1 (MUC1) by both immunofluorescence and Western Blot analysis. MUC1 expression in endometrial tissues is at the highest in secretory phases, when embryo implantation occurs and seems to protect the mucosal surface from infection and the action of degradative enzymes [32]. We observed, by immunofluorescence, a decrease in HLA-G and MUC1 expression in trophoblast spheroids co-cultured with ESC from HHV-6A positive women (**Figure 3A, upper panels**). On the contrary, the HLA-G expression was preserved in trophoblast spheroids co-cultured with ESC from HHV-6A negative women and MUC1 expression was increased (**Figure 3A, lower panels**).

The Western blot analysis conducted under reducing conditions showed the monomeric HLA-G at 39kDa and an HLA-G-like isoform at 53 kDa (Figure 4B) in all the samples, with a decrease in trophoblast spheroids co-cultured with ESC from HHV-6A positive women (**Figure 3B, upper panel**). MUC1 expression was similarly decreased in trophoblast spheroids co-cultured with ESC from HHV-6A positive women (**Figure 3B, lower panel**).

Discussion

Herein, we demonstrate for the first time that HHV-6A infection of human endometrial epithelial cells (ESC) might impair decidualisation and alter the endometrial moelcular expression. Using an *in-vitro* model, we demonstrated that HHV-6A infection attenuates ESC decidualisation.

Furthermore, HHV-6A infection caused a reduction in protein levels of the widely used phenotypic decidualisation marker, HLA-G [23] and MUC1 [32]. HLA-G is a key factor in the process of decidualisation and is thought to also be involved in endothelial cell differentiation, implantation, angiogenesis, trophoblast cell growth and immune regulation during early pregnancy. MUC1 expression in endometrial tissues is at the highest in secretory phases, when embryo implantation occurs and seems to protect the mucosal surface from infection and the action of degradative enzymes [32]. This observation is of extreme importance, since a reduction of endometrial HLA-G and MUC1 has been linked to recurrent miscarriage [23,33]. Furthermore, we show that HHV-6A infection changes the cytokine secretion profile, with an impact on endometrial immune phenotype. Interestingly, we observed a reduction in the levels of IL-15/Fn-14 and IL-18/TWEAK mRNA expression in HHV-6A negative infertile women, characterized by a low immune activation profile and reflecting a low eNK maturation and a low local angiogenesis. On the contrary, HHV-6A positive infertile women presented an over-activated immune-profile, with high IL-15/Fn-14 and IL-18/TWEK mRNA expression. We observed a lower percentage of $CD56^{bright}CD16^{-}$ (e)NK cells in women positive for HHV-6A infection, as previously observed [1] and a decrease in $CD4^{+}CD25^{+}CD127^{dim/-}$ regulatory T cells. The immune dysregulation observed in HHV-6A positive infertile women might have relevance for embryo implantation, that is controlled by endometrial immune environment [26]. It is possible that the infection could therefore lead to defective trophoblast invasion due to modification in the expression of essential attractant signalling molecules, as HLA-G and MUC1. The HLA-G isoform at 39kD is the HLA-G1 isoform. This isoform is the functional HLA-G isoform, with a recognized function at the maternal-fetal interface [34]. The HLA-G-like isoform at 53 kDa is known to be present [35] but no information is available on its function.

Alternative splicing may regulate MUC1 expression and possibly function in different cell types [36]. The isoforms identified are representative of the core protein, that has an estimated weight of 120–225 kDa, and is typical for the endometrial epithelium [37].

Our findings are also important because infertile women have been reported to have different immune cell profiles compared to fertile women [26], including increased levels of uterine natural killer cells [38] and decreased Treg cells [24]. Dysregulated immune profiles due to HHV-6A infection, as indicated in our study, could therefore also impact on the population of immune cells at the feto-maternal interface by altering immune cell recruitment.

In summary, our data suggest a novel mechanism through which HHV-6A infection leads to defective endometrial decidualisation, resulting in an altered immune response that could impact upon trophoblast migration and immune cell recruitment. Future work to clarify the potential role of HHV-6A infections upon embryo implantation and trophoblast invasion via immune dysregulation and immune cell recruitment in the endometrium due to altered immune profile could further our understanding of this potential mechanism of infection associated infertility.

References

1. Marci R, Gentili V, Bortolotti D, et al. Presence of HHV-6A in Endometrial Epithelial Cells from Women with Primary Unexplained Infertility. *PLoS One.* 2016;11(7):e0158304.
2. Takahashi K, Sonoda S, Higashi K, et al. Predominant CD4 T-lymphocyte tropism of human herpesvirus 6-related virus. *Journal of virology.* 1989;63(7):3161-3163.

3. Sandhoff T, Kleim JP, Schneweis KE. Latent human herpesvirus-6 DNA is sparsely distributed in peripheral blood lymphocytes of healthy adults and patients with lymphocytic disorders. *Medical microbiology and immunology.* 1991;180(3):127-134.

4. Ablashi D, Agut H, Alvarez-Lafuente R, et al. Classification of HHV-6A and HHV-6B as distinct viruses. *Archives of virology.* 2014;159(5):863-870.

5. Yamanishi K, Okuno T, Shiraki K, et al. Identification of human herpesvirus-6 as a causal agent for exanthem subitum. *Lancet.* 1988;1(8594):1065-1067.

6. Soldan SS, Berti R, Salem N, et al. Association of human herpes virus 6 (HHV-6) with multiple sclerosis: increased IgM response to HHV-6 early antigen and detection of serum HHV-6 DNA. *Nature medicine.* 1997;3(12):1394-1397.

7. McCullers JA, Lakeman FD, Whitley RJ. Human herpesvirus 6 is associated with focal encephalitis. *Clinical infectious diseases : an official publication of the Infectious Diseases Society of America.* 1995;21(3):571-576.

8. Grivel JC, Santoro F, Chen S, et al. Pathogenic effects of human herpesvirus 6 in human lymphoid tissue ex vivo. *Journal of virology.* 2003;77(15):8280-8289.

9. Lusso P, Markham PD, Tschachler E, et al. In vitro cellular tropism of human B-lymphotropic virus (human herpesvirus-6). *The Journal of experimental medicine.* 1988;167(5):1659-1670.

10. Lusso P, De Maria A, Malnati M, et al. Induction of CD4 and susceptibility to HIV-1 infection in human CD8+ T lymphocytes by human herpesvirus 6. *Nature.* 1991;349(6309):533-535.

11. Lusso P, Gallo RC. Human herpesvirus 6. *Bailliere's clinical haematology.* 1995;8(1):201-223.

12. Kakimoto M, Hasegawa A, Fujita S, Yasukawa M. Phenotypic and functional alterations of dendritic cells induced by human herpesvirus 6 infection. *Journal of virology.* 2002;76(20):10338-10345.

13. Smith AP, Paolucci C, Di Lullo G, Burastero SE, Santoro F, Lusso P. Viral replication-independent blockade of dendritic cell maturation and interleukin-12 production by human herpesvirus 6. *Journal of virology.* 2005;79(5):2807-2813.

14. Smith A, Santoro F, Di Lullo G, Dagna L, Verani A, Lusso P. Selective suppression of IL-12 production by human herpesvirus 6. *Blood.* 2003;102(8):2877-2884.

15. Flamand L, Gosselin J, Stefanescu I, Ablashi D, Menezes J. Immunosuppressive effect of human herpesvirus 6 on T-cell functions: suppression of interleukin-2 synthesis and cell proliferation. *Blood.* 1995;85(5):1263-1271.

16. Flamand L, Gosselin J, D'Addario M, et al. Human herpesvirus 6 induces interleukin-1 beta and tumor necrosis factor alpha, but not interleukin-6, in peripheral blood mononuclear cell cultures. *Journal of virology.* 1991;65(9):5105-5110.

17. Janelle ME, Flamand L. Phenotypic alterations and survival of monocytes following infection by human herpesvirus-6. *Archives of virology.* 2006;151(8):1603-1614.

18. Beer AE, Kwak JY, Ruiz JE. Immunophenotypic profiles of peripheral blood lymphocytes in women with recurrent pregnancy losses and in infertile women with multiple failed in vitro fertilization cycles. *Am J Reprod Immunol.* 1996;35(4):376-382.

19. Quenby S, Bates M, Doig T, et al. Pre-implantation endometrial leukocytes in women with recurrent miscarriage. *Human reproduction.* 1999;14(9):2386-2391.

20. Kwak-Kim J, Gilman-Sachs A. Clinical implication of natural killer cells and reproduction. *Am J Reprod Immunol.* 2008;59(5):388-400.

21. Rizzo R, Bortolotti D, Bolzani S, Fainardi E. HLA-G Molecules in Autoimmune Diseases and Infections. *Frontiers in immunology.* 2014;5:592.

22. Kovats S, Main EK, Librach C, Stubblebine M, Fisher SJ, DeMars R. A class I antigen, HLA-G, expressed in human trophoblasts. *Science.* 1990;248(4952):220-223.

23. Rizzo R, Vercammen M, van de Velde H, Horn PA, Rebmann V. The importance of HLA-G expression in embryos, trophoblast cells, and embryonic stem cells. *Cell Mol Life Sci.* 2011;68(3):341-352.

24. Kofod L, Lindhard A, Hviid TVF. Implications of uterine NK cells and regulatory T cells in the endometrium of infertile women. *Human immunology.* 2018;79(9):693-701.

25. Morandi F, Venturi C, Rizzo R, et al. Intrathecal soluble HLA-E correlates with disease activity in patients with multiple sclerosis and may cooperate with soluble HLA-G in the resolution of neuroinflammation. *J Neuroimmune Pharmacol.* 2013;8(4):944-955.

26. Ledee N, Petitbarat M, Chevrier L, et al. The Uterine Immune Profile May Help Women With Repeated Unexplained Embryo Implantation Failure After In Vitro Fertilization. *Am J Reprod Immunol.* 2016;75(3):388-401.

27. Caselli E, Zatelli MC, Rizzo R, et al. Virologic and immunologic evidence supporting an association between HHV-6 and Hashimoto's thyroiditis. *PLoS Pathog.* 2012;8(10):e1002951.

28. Caselli E, Bortolotti D, Marci R, et al. HHV-6A Infection of Endometrial Epithelial Cells Induces Increased Endometrial NK Cell-Mediated Cytotoxicity. *Front Microbiol.* 2017;8:2525.

29. Cai J, Peng T, Wang J, et al. Isolation, Culture and Identification of Choriocarcinoma Stem-Like Cells from the Human Choriocarcinoma Cell-Line JEG-3. *Cellular physiology and biochemistry : international journal of experimental cellular physiology, biochemistry, and pharmacology.* 2016;39(4):1421-1432.

30. Fainardi E, Bortolotti D, Bolzani S, et al. Cerebrospinal fluid amounts of HLA-G in dimeric form are strongly associated to patients with MRI inactive multiple sclerosis. *Multiple sclerosis.* 2016;22(2):245-249.

31. Rizzo R, Lo Monte G, Bortolotti D, et al. Impact of soluble HLA-G levels and endometrial NK cells in uterine flushing samples from primary and secondary unexplained infertile women. *Int J Mol Sci.* 2015;16(3):5510-5516.

32. McAuley JL, Corcilius L, Tan HX, Payne RJ, McGuckin MA, Brown LE. The cell surface mucin MUC1 limits the severity of influenza A virus infection. *Mucosal immunology.* 2017;10(6):1581-1593.

33. Wu F, Chen X, Liu Y, et al. Decreased MUC1 in endometrium is an independent receptivity marker in recurrent implantation failure during implantation window. *Reproductive biology and endocrinology : RB&E.* 2018;16(1):60.

34. Rizzo R, Vercammen M, van de Velde H, Horn PA, Rebmann V. The importance of HLA-G expression in embryos, trophoblast cells, and embryonic stem cells. *Cellular and Molecular Life Sciences*. 2011;68(3):341-352.

35. Gonzalez A, Alegre E, Arroyo A, LeMaoult J, Echeveste JI. Identification of circulating nonclassic human leukocyte antigen G (HLA-G)-like molecules in exudates. *Clinical Chemistry* 2011;57(7):1013-22.

36 Zhang L, Vlad A, Milcarek C, Finn OJ. Human Mucin MUC1 RNA Undergoes Different Types of Alternative Splicing Resulting in Multiple Isoforms. *Cancer Immunology, Immunothererapy* 2013;62(3): 423–435.

37. Lagow E, DeSouza MM, Carson DD. Mammalian reproductive tract mucins. *Human Reproduction Update* 1999;5(4):280-92.

38. Yougbare I, Tai WS, Zdravic D, et al. Activated NK cells cause placental dysfunction and miscarriages in fetal alloimmune thrombocytopenia. *Nat Commun.* 2017;8(1):224.

Table 1. Women cohorts: demographical and clinical parameters

Parameters (medain; mean±SD)	Infertile (67)	Fertile (100)	p value †
Age (yrs)	34.6 (33.2±2.2)	33.8 (32.5±2.9)	0.97
Duration of infertility (yrs)	3.5 (3.6±2.9)	-	-
Length of menstrual cycle (days)	28 (25±2.9)	29 (26±315)	0.56
FSH (mUI/mL) (day 3)	7.7 (7.9±1.8)	7.5 (7.6±2.7)	0.54
LH (mUI/mL) (day 3)	6.7 (6.8±2.3)	7.1 (6.5±2.5)	0.53
Estradiol (pg/mL) (day 3)	71.4 (72.1±53.5)	63.4 (58.6±47.2)	0.054
TSH (uUI/mL)	3.1 (2.8±2.5)	2.9 (2.6±2.4)	0.51
FT4 (pg/mL)	2.3 (2.3±1.6)	2.4 (2.5±1.6)	0.92
Progesterone (pg/mL) (day 21)	14.9 (14.5±5.2)	14.8 (14.3±6.4)	0.72
Smoke habits (≥1 cigarette/day) (%)‡	32	53	0.45
Day (mestrual cycle) of sample collection	14.0 (13.1±2.3)	14.1 (13.4±2.6)	0.97

†Student T test

‡ Fisher exact test

Table 2. HHV-6 DNA results in peripheral blood mononuclear cells (PBMC) and endometrial biopsies

Samples (N)	Infertile (67)	Fertile (100)	p value†
HHV6-A			
Endometrial epithelium	27‡	0	<0.0001
Endometrial stroma	0	0	NA
Endometrial leukocytes (CD45pos)	0	0	NA
PBMC	0	0	NA
HHV-6B			
Endometrial epithelium	0	0	NA
Endometrial stroma	0	0	NA
Endometrial leukocytes (CD45pos)	0	0	NA
PBMC	17	24	0.856

†Fisher exact test

‡ (range 710.000–189.000 copies/ug DNA)

Table 3. Comparison of endometrial biomarkers in fertile and infertile women.

	Fertile group N=100	**Infertile group N=67**	
Biomarkers		**HHV-6A pos N=27**	**HHV-6A neg N=40**
IL-18/TWEAK	0.081±0.021	0.15±0.04	0.015±0.022
IL-15/Fn-14	1.3±0.56	3.2±0.69	0.25±0.12

The values are reported as mean±SD.

Figure legends

Figure 1. A) eNK cell subpopulations $CD56^{bright}$ (left panel) and $CD556^{dim}$ (right panel); B) peripheral blood immune cells. Results are expressed in cells/ul; C) Percentage of

$CD4^+CD25^+CD127^{dim/-}$ regulatory T cells in peripheral blood. Each data point is calculated as the mean ± S.D. Significant p-values are reported (Student T test).

Figure 2. Co-culture model to mimic the trophoblast– decidual interface in early pregnancy. Spheroids were formed from the trophoblast cell line JEG-3 and placed onto a monolayer of epithelial-stromal cells (ESC) in a 1:1 ratio from HHV-6A positive and negative women. A representative result is reported from the beginning of the observation period (T0), after 2 days (T2) and 3 days (T3). To visualize the spheroid contours, Syto 59 staining for the JEG3 spheroids was performed at the beginning of the observation period (T0). The area covered by each individual spheroid was determined at the beginning (T0) and at the end (T3) of the co-culture period. In the lower panel, the spheroid expansion is reported relative to T0. The ratio between T3 and T0 area (T3 area/T0 area), calculated by Nikon Nis-Elements (Nikon Italy) was used to evaluate the modification in spheroid dimensions. Each data point is calculated as the mean ± S.D. Significant p-values are reported (Student T test). Images were taken in fluorescence (Nikon Eclipse TE2000S) equipped with a digital camera. Original magnification 20x and 40x.

Figure 3. Impact of 3 days co-culture of ESC with trophoblast spheroid on trophoblast molecular expression. We analyzed the expression of HLA-G and mucin-1 (MUC1) by both A) immunofluorescence, where images were taken in bright field (*left panels*) or fluorescence (*right panels*) (Nikon Eclipse TE2000S) equipped with a digital camera and an original magnification 20x; and B) Western Blot analysis, conducted under reducing conditions. For HLA-G the arrows indicate the monomeric HLA-G at 39kDa and an HLA-G-like isoform at 53 kDa while in MUC1 the arrows indicate the MUC1 120kDa and an isoform at 240 kDa, that depends on glycosylation level. The densitometric analysis is reported as fold changes of the most representative and functional isoforms HLA-G (39kDa) or MUC1(120kDa) expression relative to T0. Each data point is calculated as the mean ± S.D. Significant p-values are reported (Student t test).

Supplementary Figures

Figure 1. A) Epithelial and stromal cell fraction derived by immunomagnetic separation was characterized by immunofluorescence for cytokeratin18 (CK18) and vimentin expression, respectively. Images were taken in bright field (*left panels*) or fluorescence (*right panels*) (Nikon Eclipse TE2000S) equipped with a digital camera. Original magnification 20×. **B)** HHV-6 DNA was searched by real-time qPCR specific for U94 gene in endometrial biopsies. Results are expressed in viral copies/ug DNA and represent the mean copy number ± SD referred to duplicates of 2 independent assays. **C)** Representative dot plot of eNK cells obtained from endometrial biopsies from HHV-6A positive and negative infertile women. eNK cells were stained with CD3-AmCyan (Clone SK7), CD16-APCCy7 (Clone B73.1), CD56-PE (Clone CMSSB) monoclonal antibodies. Cells were gated to be $CD3^-$.

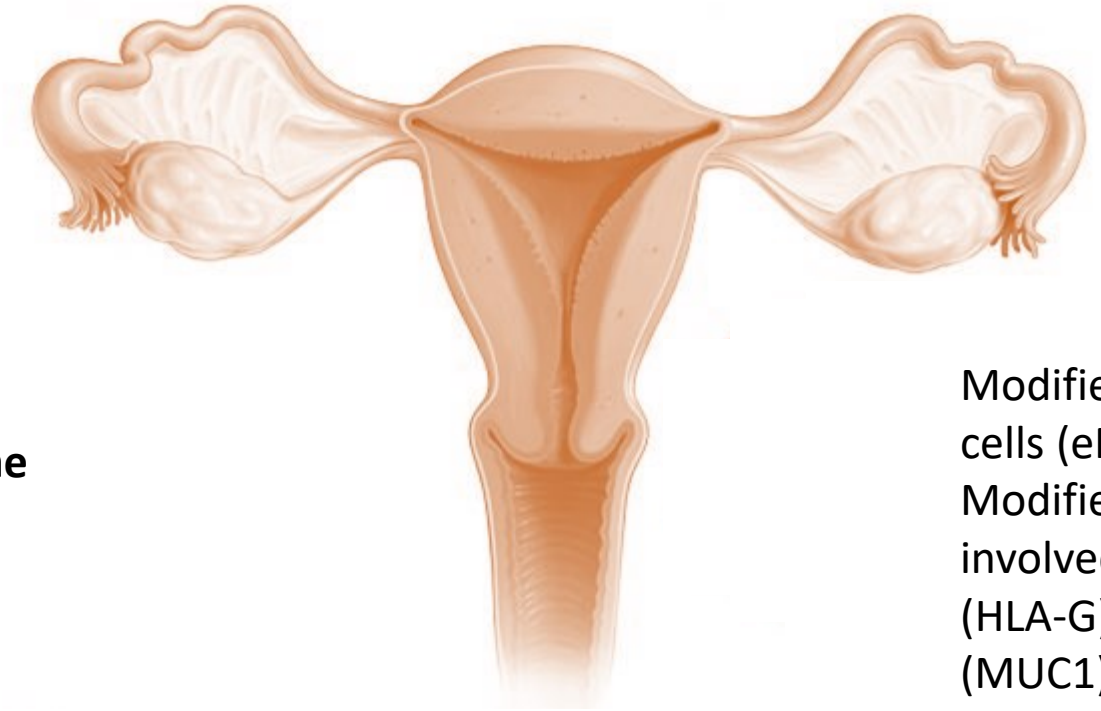

Endometrial Biodiversity

Endometrial virome
HHV-6A infection
HHV-6A spreading

Modified percentage of immune cells (eNK; Treg)
Modified expression of proteins involved into immune regulation (HLA-G) and infection control (MUC1)

Endometrial immune system

Relationship between microorganisms and host

Altered immune response

Implantation rate
Pregnancy rate
Ongoing pregancy
Live-birth rate

A)

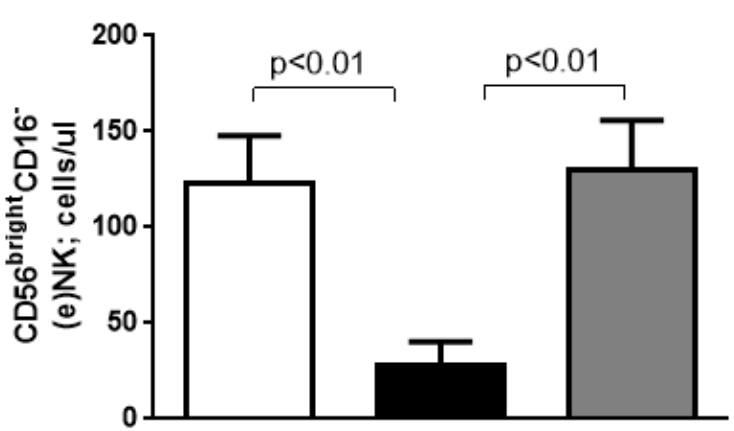
200
150
100
50
0
p<0.01
p<0.01
CD56bright CD16- (e)NK; cells/ul

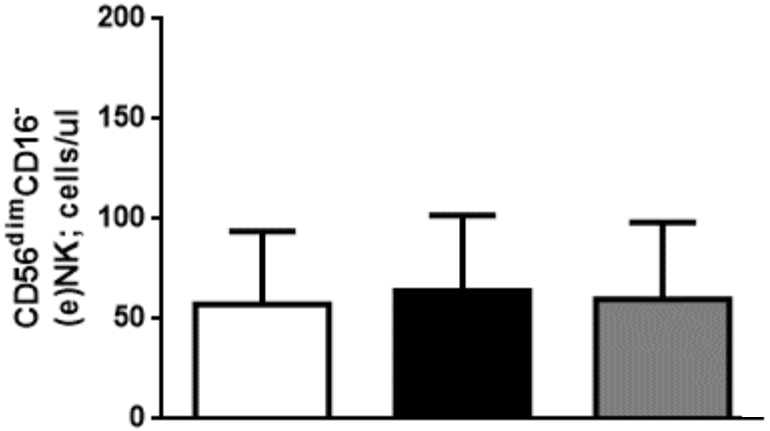
200
150
100
50
0
CD56dim CD16- (e)NK; cells/ul

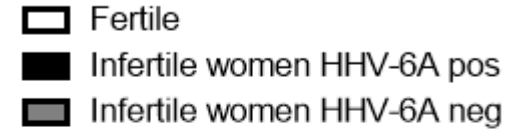
Fertile
Infertile women HHV-6A pos
Infertile women HHV-6A neg

B)

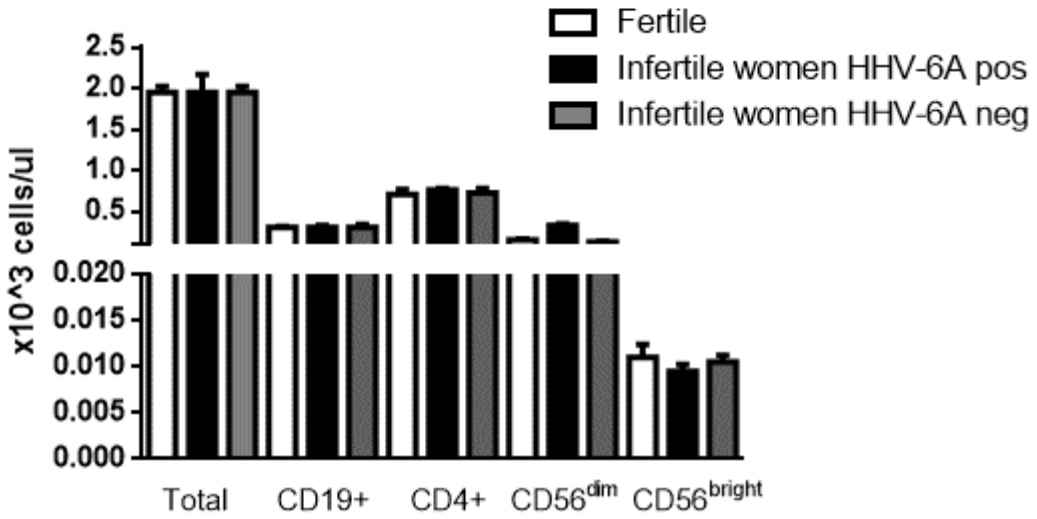
Fertile
Infertile women HHV-6A pos
Infertile women HHV-6A neg
x10^3 cells/ul
2.5
2.0
1.5
1.0
0.5
0.020
0.015
0.010
0.005
0.000
Total
CD19+
CD4+
CD56dim
CD56bright

C)

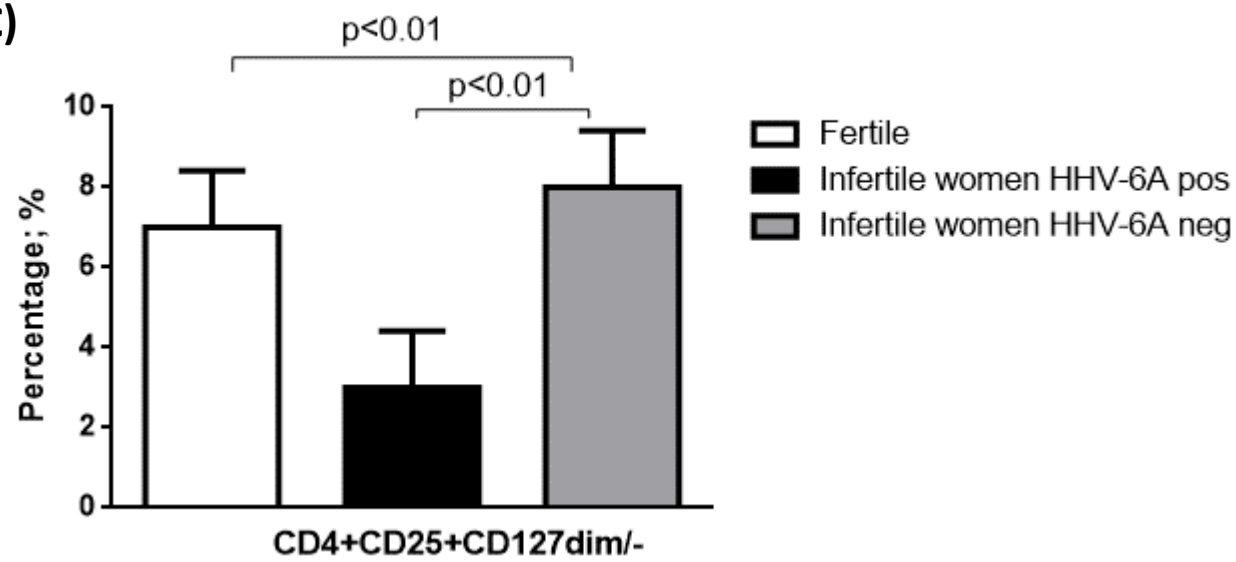
p<0.01
p<0.01
10
8
6
4
2
0
Percentage; %
CD4+CD25+CD127dim/-
Fertile
Infertile women HHV-6A pos
Infertile women HHV-6A neg

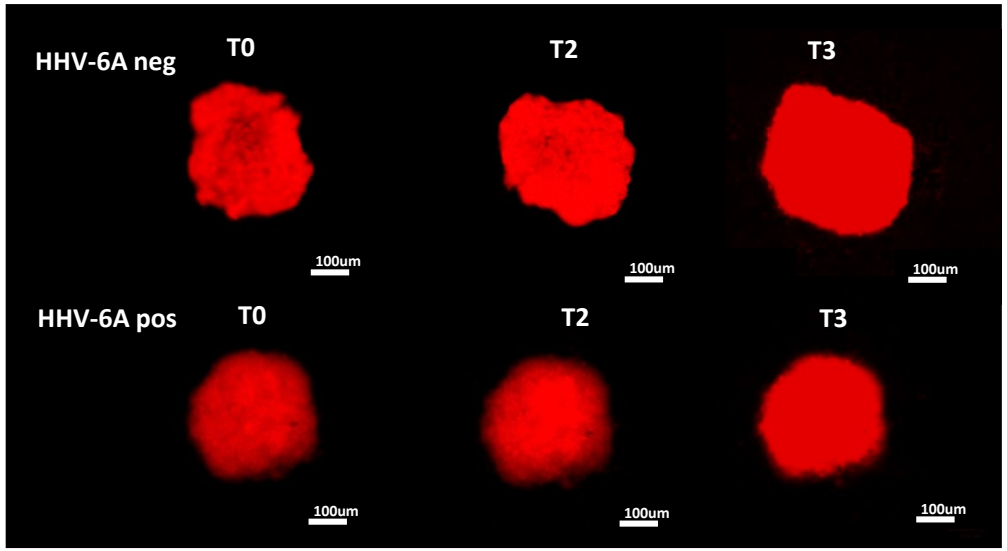
HHV-6A neg
T0
T2
T3
100um
100um
100um
HHV-6A pos
T0
T2
T3
100um
100um
100um

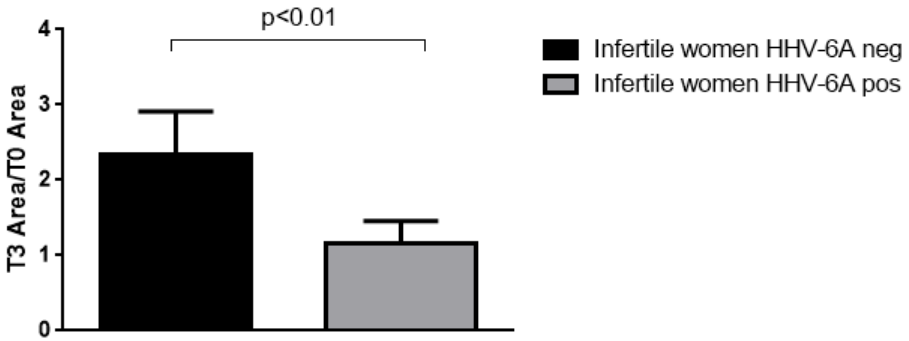
p<0.01
T3 Area/T0 Area
0
1
2
3
4
Infertile women HHV-6A neg
Infertile women HHV-6A pos

A)

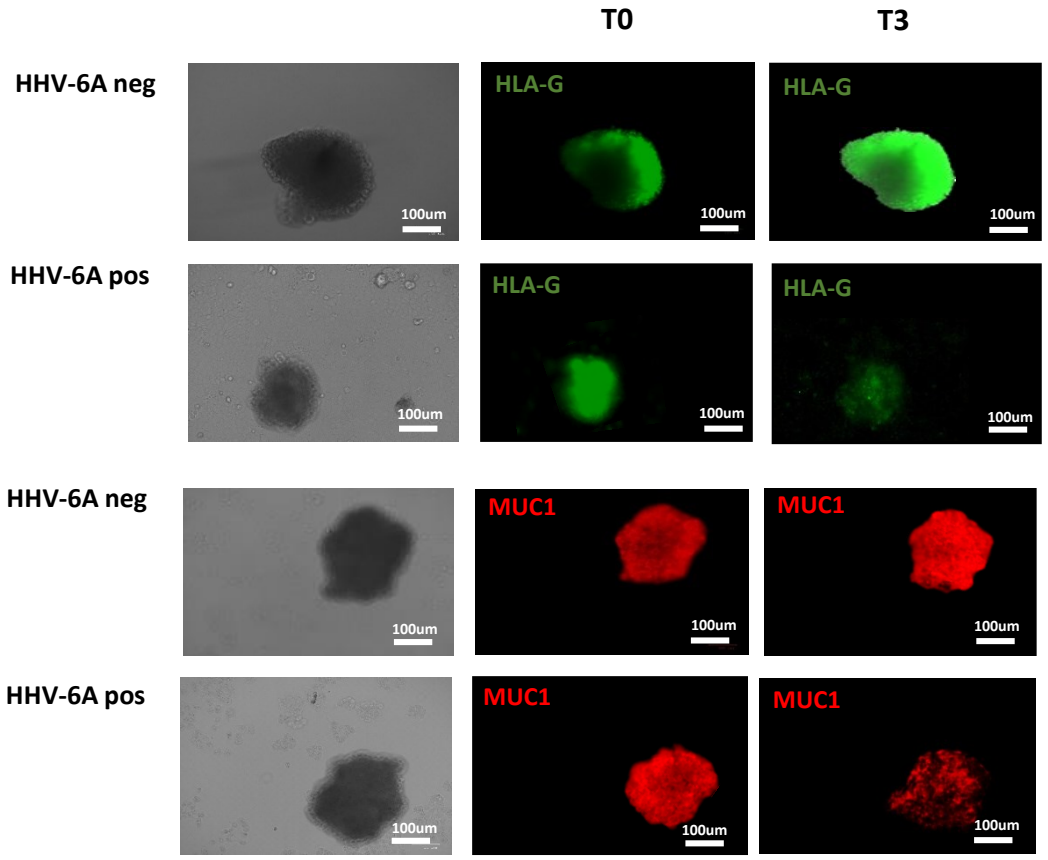
T0
T3
HHV-6A neg
HLA-G
HLA-G
HHV-6A pos
HLA-G
HLA-G
HHV-6A neg
MUC1
MUC1
HHV-6A pos
MUC1
MUC1
100um

B)

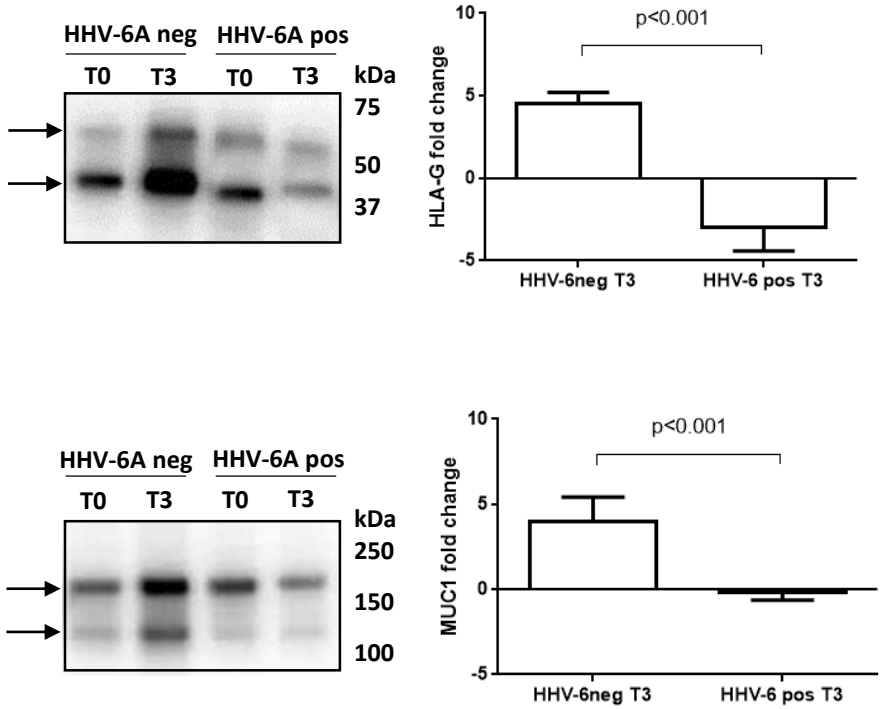
HHV-6A neg
HHV-6A pos
T0
T3
T0
T3
kDa
75
50
37
p<0.001
HLA-G fold change
10
5
0
-5
HHV-6neg T3
HHV-6 pos T3
HHV-6A neg
HHV-6A pos
T0
T3
T0
T3
kDa
250
150
100
p<0.001
MUC1 fold change
10
5
0
-5
HHV-6neg T3
HHV-6 pos T3

A)

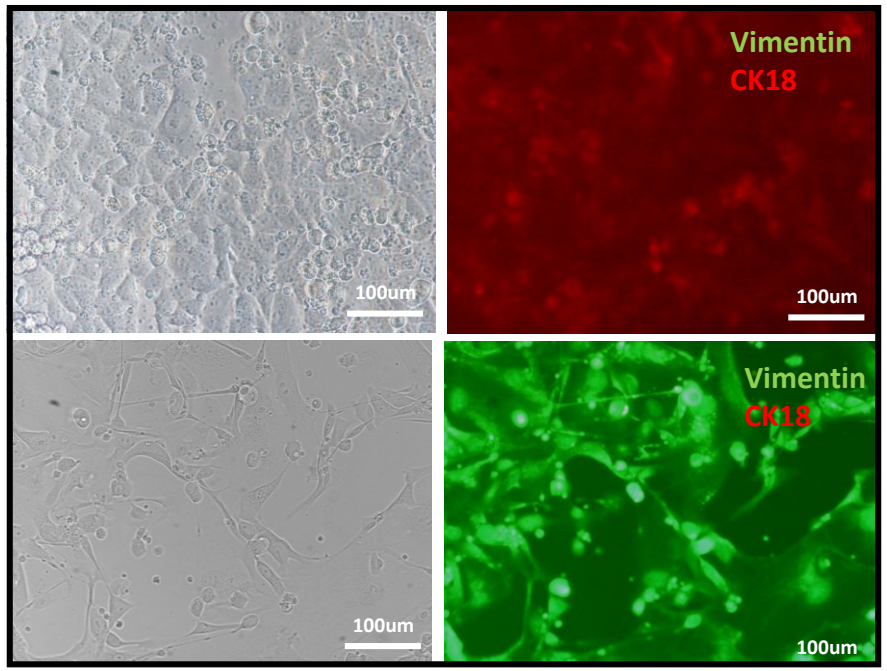
Vimentin
CK18
100um
100um
100um
Vimentin
CK18
100um

B)

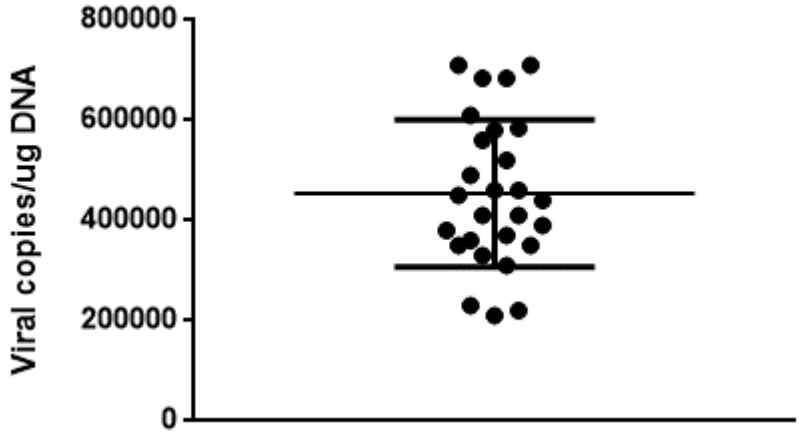
Viral copies/ug DNA
800000
600000
400000
200000
0

C)

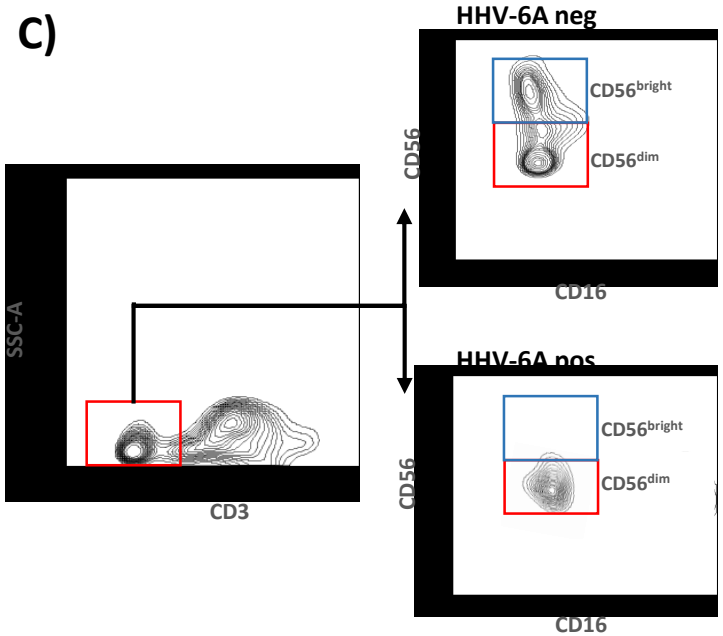
HHV-6A neg
CD56bright
CD56dim
CD56
CD16
SSC-A
CD3
HHV-6A pos
CD56bright
CD56dim
CD56
CD16